Measuring Traction Forces of Motile Dendritic Cells on Micropost Arrays

Brendon G. Ricart,[†] Michael T. Yang,[‡] Christopher A. Hunter,[§] Christopher S. Chen,[†‡] and Daniel A. Hammer[†‡*]
[†]Department of Chemical and Biomolecular Engineering, [‡]Department of Bioengineering, and [§]Department of Pathobiology, University of Pennsylvania, Philadelphia, Pennsylvania

ABSTRACT Dendritic cells (DCs) migrate from sites of inflammation to secondary lymphoid organs where they initiate the adaptive immune response. Although motility is essential to DC function, the mechanisms by which they migrate are not fully understood. We incorporated micropost array detectors into a microfluidic gradient generator to develop what we consider to be a novel method for probing low magnitude traction forces during directional migration. We found migration of primary murine DCs is driven by short-lived traction stresses at the leading edge or filopodia. The traction forces generated by DCs are smaller in magnitude than found in neutrophils, and of similar magnitude during chemotaxis and chemokinesis, at 18 ± 1.4 and 16 ± 1.3 nN/cell, respectively. The characteristic duration of local DC traction forces was 3 min. The maximum principal stress in the cell occurred in the plane perpendicular to the axis of motion, forward of the centroid. We illustrate that the spatio-temporal pattern of traction stresses can be used to predict the direction of future DC motion. Overall, DCs show a mode of migration distinct from both mesenchymal cells and neutrophils, characterized by rapid turnover of traction forces in leading filopodia.

INTRODUCTION

Dendritic cells (DCs) are potent initiators of the adaptive immune response. These cells are stationed throughout the periphery awaiting pathogen entry, after which they mature and migrate to lymph nodes where they orchestrate lymphocyte activation (1). To perform their function, DCs must interpret external cues to allow them to migrate through a series of varied microenvironments. For example, DCs are chemotactic toward soluble CCL19 and bound CCL21 (2), use actin polymerization and myosin contraction for locomotion (3), and are readily adaptable to migration on adhesive and nonadhesive substrates (4). Although recent studies have focused on the mechanics of DC migration (5,6), their traction force profiles remain unknown. Because these cells are central to the functioning of the immune system, elucidating the molecular mechanisms of directional control and force generation in these cells would be key to manipulating directional homing in the immune system.

Force profiles during migration are generally classified as "amoeboid" or "lamellipodial". Initial work with DCs has classified them as amoeboid cells (4,5,7) based on their high degree of motility and rapidly changing cell shape, but this has not been confirmed or challenged with traction force studies. Amoeboid cells are rapidly crawling cells that exert relatively small forces. In *Dictyostelium*, a well-studied amoeboid model, forces are strongest at the contractile rear and weaker at the protrusive front (8,9). Similarly in fish keratocytes, another common amoeboid model, forces are concentrated at the sides and rear of the moving cell, with negligible force detection at the leading edge (10,11). Initial studies of traction force profiles of neutrophils performed by Smith et al. (12) showed that these cells also concentrate their forces in the rear on an ICAM-1 surface. A subsequent study by Shin et al. (13) showed that for very short timescales on the order of a few seconds, the traction forces in neutrophils can oscillate between the rear and front of the cell. Overall, amoeboid cells move rapidly and concentrate contractile forces at the sides and rear of the migrating cell body.

In contrast, lamellipodial migration is slow and characterized by nascent adhesions at the leading edge, which mature into focal adhesions and eventually disassemble at the trailing edge (14). This generates a force profile of relatively strong contractile forces under the lamellipod associated with growing adhesions (15,16), and detachment forces in the uropod as mature adhesions are released from the substratum (17). Cell types that fit the lamellipodial migration profile generally include mesenchymal cells such as fibroblasts (15,18,19), smooth muscle cells (20), epithelial cells (21–23), endothelial cells (24,25), and stem cells (26).

In previous reports of spatial orientation of traction forces, the most common assay technique has been polyacrylamide gels embedded with nanoscale fluorescent beads. Bead displacements can be correlated to traction forces imposed on the gel (16). These gels have sufficient resolution for measuring forces exerted by strongly adherent cells such as fibroblasts (16) or endothelial cells (27), making them suitable for studying lamellipodial migration. Although the forces of amoeboid cells like neutrophils have also been quantified with polyacrylamide gels, efforts to use this technology to resolve the traction forces exerted by DCs were unsuccessful as these cells are substantially weaker than neutrophils (12,28). Therefore, to study DC force generation, we used the micropost array detector (mPAD),

Submitted July 15, 2011, and accepted for publication September 8, 2011.

*Correspondence: hammer@seas.upenn.edu

Editor: Alissa Weaver.

0006-3495/11/12/2620/9 $2.00

doi: 10.1016/j.bpj.2011.09.022

which has greater sensitivity than gel-based traction force microscopy (20,29).

To measure forces during dendritic cell chemotaxis, cells were cultured on fibronectin-coated mPADs inside a microfluidic gradient generator (30), and presented with a 0.2 nM/cell gradient of CCL19; the micropost array had an effective elasticity of 1.5 kPa. Using this system, we found that dendritic cells concentrated their strongest forces at the leading edge. We find that the line of maximal stress can be used to predict the direction of motion. Additionally, the force on a micropost has a characteristic timescale that can be positively correlated to the force on that post. Finally, actomyosin inhibitors significantly depleted force generation, but not directional navigation. Conversely, pertussis toxin (PTX) blocked navigation but did not affect traction forces, indicating these components of migration may be regulated independently. This study represents, to our knowledge, the first elucidation of traction stresses in dendritic cells, describes an alternative force profile for ameboid movement, and illustrates mPAD arrays as useful detectors for motile forces in fast moving cells that generate weak forces.

MATERIALS AND METHODS

The experimental methods and protocols are described here briefly with a more detailed description included in the Supporting Material. The polydimethylsiloxane (PDMS) microfluidic gradient generator was fabricated as described previously (30). PDMS micropost arrays on glass coverslips were fabricated as in Tan et al. (20). The effective stiffness of the microposts (~1.5 kPa) was on the order of mammalian tissue. The tips of the microposts were microcontact-printed with fibronectin to promote cell adhesion. Then the micropost array substrate was bonded to the microfluidic gradient generator using oxygen plasma treatment. Once assembled, the device was perfused with ethanol followed by DiI lipophilic dye to fluorescently label the microposts. The shafts of the posts were then blocked with Pluronic F127 (BASF, Florham Park, NJ) to prevent cells from crawling down the gaps between posts. Murine dendritic cells (DCs) were obtained by culturing stem cells harvested from mouse femurs for seven days in the presence of granulocyte-macrophage colony-stimulating factor and then matured for 24 h in the presence of lipopolysaccharide. For experiments, DCs were perfused into the microfluidic device and allowed to adhere to the microposts for 10 min before timelapse images of the cells and underlying microposts were acquired.

Pharmacological inhibition of cells, if any, was performed for 1 h (blebbistatin and Latrunculin A) or 24 h (PTX) before the experiment. In all experiments, chemotaxis was driven by a linear soluble gradient of 0–20 nM CCL19. The force exerted by DCs on each post was determined by a custom-written MATLAB (The MathWorks, Natick, MA) script (21). Briefly, acquired timelapse images were rotated and registered, a region of interest was defined, and the centroids of the posts were automatically determined. The cells were outlined to follow their movement over posts within the region of interest. Forces were then computed by multiplying the displacements of attached posts with the spring constant of the microposts, which is 1.9 nN/μm. The lines of maximal stress and front-rear distribution of forces were calculated using custom-made MATLAB software). To determine the timescale of single-post deflections, half-max full-width analysis was performed on the raw post-displacement data. The timescales of post deflections were fit to a log-normal distribution to extract the mean and median values.

RESULTS AND DISCUSSION

DC migration on micropost surfaces

We measured the motility of dendritic cells on fibronectin-coated micropost arrays of 1.5 kPa elasticity, in the presence and absence of chemokine gradients. During chemokinesis, in the absence of a chemokine gradient, DCs migrated randomly at an average velocity of 2.3 $\pm$ 0.5 μm/min on the micropost array (see Movie S1 in the Supporting Material), similar to their velocity on other substrates (2,5,31). The random motility coefficient on the mPAD surface was 48 μm^2/min, slightly lower than on glass substrates (30). Because substrate mechanics often affect migration parameters, this difference may be due to the reduced perceived stiffness of the substrate (32). During chemokinesis, we measured the average strain energy over the cell to be 2.4 $\pm$ 0.6 fJ. Overall, DC migration was not significantly altered by the micropost surface.

Next, we used a microfluidic gradient generator in combination with the micropost array surface to present DCs with a chemokine gradient while monitoring their traction forces (Fig. 1, and see Movie S2). We found that DCs concentrate integrin-based contractile forces at the leading edge, with almost no force at the trailing edge (Fig. 2 *A*). This pulling force is often characterized by a highly localized contraction of two to three microposts in which the net force is always pulling toward the nucleus. This force must be counterbalanced at the rear, and we observed these counterbalancing forces to be diffuse, weak adhesions under the cell body. The average force on a micropost exerted by DCs during chemotaxis was 0.55 $\pm$ 0.4 nN, giving rise to a total cellular strain energy of 2.6 $\pm$ 0.2 fJ (Fig. 2, *E* and *F*).

DC forces depend on actomyosin, but not gradient sensing

The key components of cell motility are actin-based polymerization, myosin-based contraction, integrin-based adhesion, and GPCR-based signaling/polarity (5). To disrupt actin polymerization, we used the chemical inhibitor Latrunculin A. In the absence of actin polymerization, motility was completely abrogated (Fig. 2, *C* and *G*, and see Movie S3), and force transmission to the microposts was minimal (Fig. 2, *C*, *E*, and *F*) as cells failed to spread on the substrate (Fig. 2 *I*). After treatment with blebbistatin to disrupt myosin II-based contractility, cells displayed slower speeds (Fig. 2 *G*) and >50% reduction in traction forces (Fig. 2, *B*, *E*, and *F*, and see Movie S4). We also used PTX to disrupt chemokine signaling from the extracellular gradient (Fig. 2 *H*). This treatment gave only a slight reduction in force per post (Fig. 2 *F*, and see Movie S5), while the average cellular force was not affected (Fig. 2, *D* and *E*) because the treated cells had a greater spread area (Fig. 2 *I*). Taken together, these data

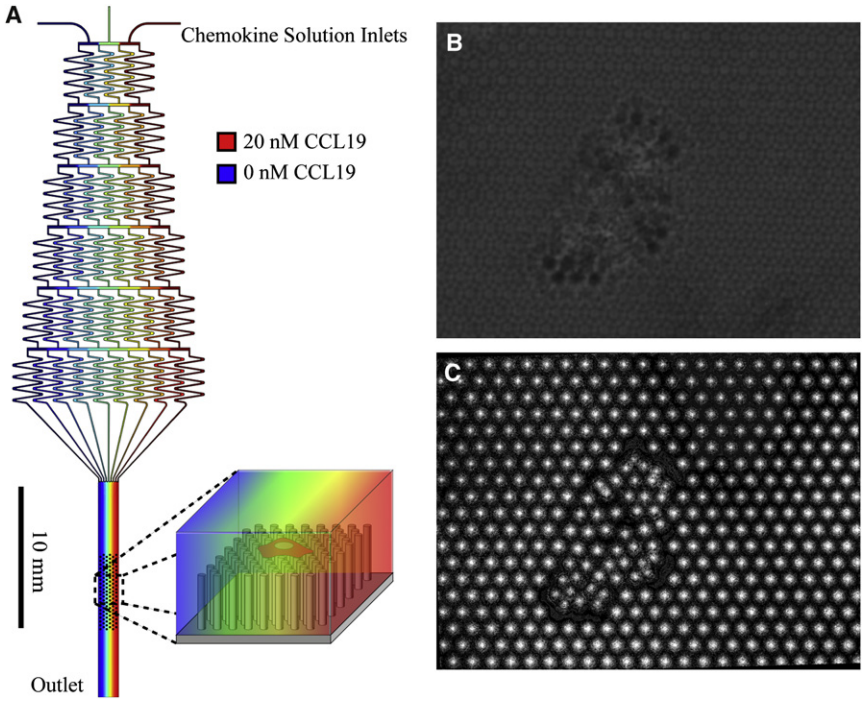

FIGURE 1 (*A*) Microfluidic gradient generator coupled to a micropost array detector. Chemokine solutions containing 20, 10, and 0 nM CCL19 are perfused into inlets at the top of the chamber at 3 μL/min/inlet. Colors in the diagram correspond to chemokine concentration (*red*, *green*, and *blue* correspond to 20, 10, and 0 nM, respectively). The three inlets are mixed in a series of microchannels forming a smooth gradient in the cell viewing region. Micropost array detector of effective stiffness 1.5 kPa forms the migration surface within the viewing region. The tips of microposts are functionalized with fibronectin and the sides are passivated with an amphiphilic triblock copolymer. The gradient presented to cells (2 K_D/mm) has been optimized to induce maximal chemotactic index. (*B* and *C*) Representative images mature dendritic cells crawling on fluorescently labeled fibronectin post arrays, imaged in phase contrast (*B*) and in fluorescence (*C*) to detect post deflections.

show that in DCs, traction force and speed are correlated, but traction forces are somewhat independent of gradient sensing.

DC traction stresses are concentrated at the leading edge

Because dendritic cells form individual adhesions on each attached micropost during locomotion (5), we were able to directly measure the contractile stresses exerted through distinct adhesions. We found that traction forces are stronger under the leading edge than either the nucleus or the rear of the cell. This was quantified by finding the line of maximal stress along the axis of motion (Fig. 3 *A*, *dashed line*). The axis of motion was determined by the vector from the current cell centroid to the next cell centroid, ~3 min later. Because contractile force transmitted through adhesions is generally directed inward, if forces are strongest at the front we should expect diffuse counterbalancing forces under the trailing cell body resulting in maximal stress in front of the cell centroid. For DCs, we find that the line of maximal stress is typically located in front of the cell centroid (Fig. 2 *A* and Fig. 3 *B*). Even when gradient sensing was lost by PTX inhibition, the point of maximal stress was still generally in front of the centroid (Fig. 3 *C*), meaning that forces are still concentrated at the leading edge in the absence of asymmetric GPCR signaling. Treatment with actomyosin inhibitors greatly reduced traction stresses, and shifted the point of maximal stress toward the cell centroid (Fig. 3, *D* and *E*), leading to the loss of directional information in the migrating cell.

DC tractions stresses predict direction of motion

Using a single traction map, the direction of motion can be predicted a priori. As a prediction, we searched the traction map for the dividing line across which there was maximal stress (Fig. 4 *A*, *black line*), and compared it to the line perpendicular to the observed direction the cell moved over the next 5 min. The angle subtended by these lines (Θ) describes the agreement between our proposed prediction and experimental outcome. For mature dendritic cells migrating in a strong gradient of CCL19 (Fig. 4 *B*), we found that Θ is small (Fig. 4 *C*), indicating that the line of global maximal stress is close to perpendicular to the direction of motion. Combined with information about the cell centroid, this line gives accurate predictions for the direction of motion. Again, when PTX is used to disrupt gradient perception and induce random migration, the line of maximal stress still predicts the direction of motion, though with less accuracy, as Θ is not as tightly distributed at ~0 and 180° (Fig. 4 *D*). Actomyosin inhibitors further widen the distribution of Θ, decreasing the sensitivity of the prediction, but the maximal stress may still be used to give a rough indication of directionality (Fig. 4, *E* and *F*). We propose that a global search of the traction stresses from a snapshot in time can be used to predict the direction of dendritic cell migration.

Temporal duration of dendritic cell traction stresses

DCs are highly motile amoeboid cells, moving on small timescales when compared to epithelial cells or fibroblasts.

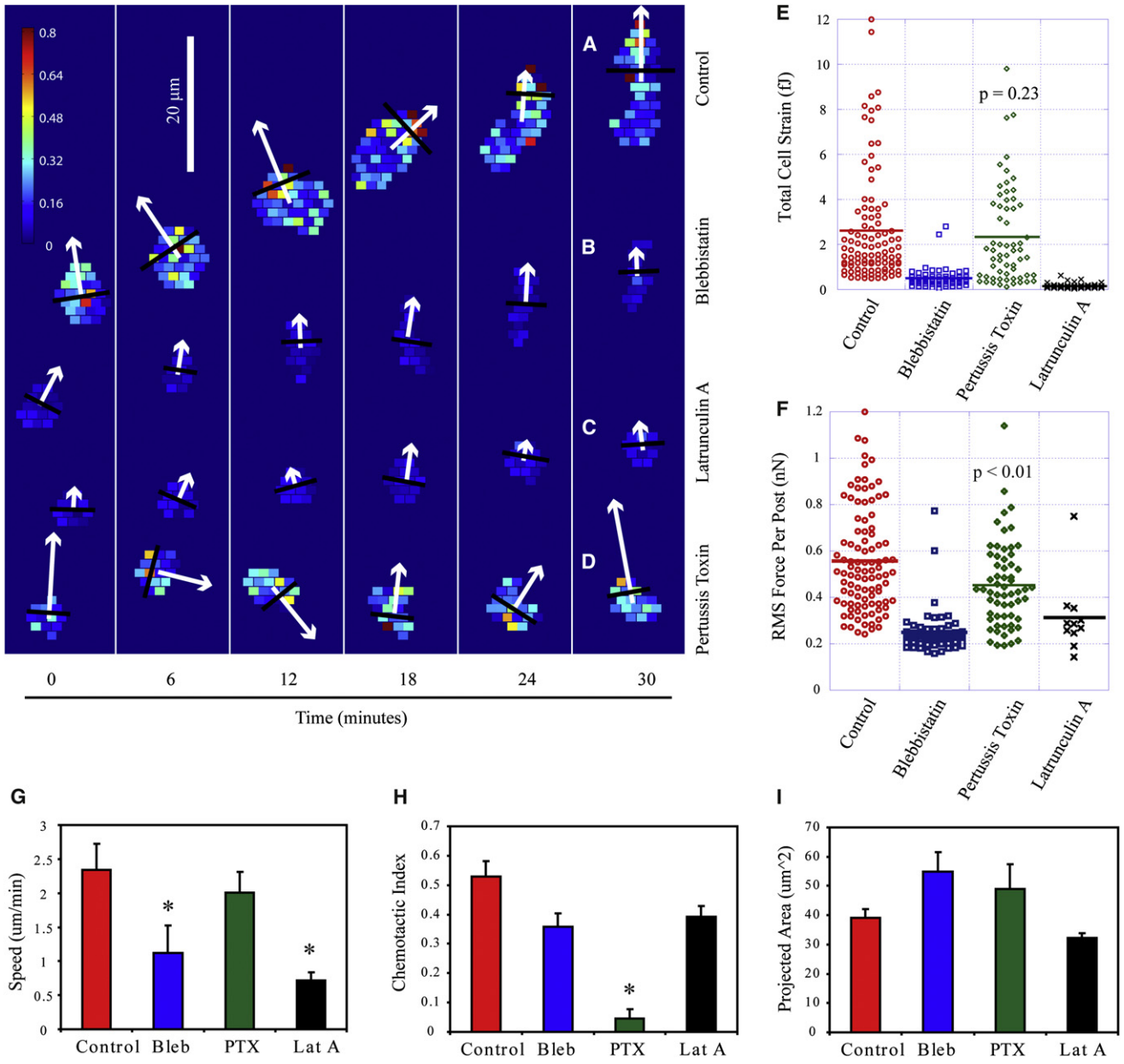

FIGURE 2 DCs migrating in a chemokine gradient concentrate traction forces at the leading edge. (*A*) A representative trace of a DC following an extracellular gradient of soluble CCL19 (highest at *top*). Each colored box underneath the cell represents a single micropost. The magnitude of the force on the micropost is shown on a colorscale of 0 (*dark blue*) to 0.8 nN (*dark red*). Cell images (*left* to *right*) are displayed at 6-min intervals, and displacement from the previous image is scaled according to the scale bar. Cell trajectories (*white arrows*) show direction and speed of displacement. The line of maximal stress normal to the direction of motion (*black lines*) is typically in front of the cell centroid. (*B–D*) Representative traces of DCs treated with blebbistatin (*B*), Latrunculin A (*C*), or pertussis toxin (PTX) (*D*) under the same conditions as panel *A*. (*E* and *F*) Total cellular strain energy and root-mean squared force per post generated by cells in a chemokine gradient. Each data point represents a single cell image ($N = 10$ per condition, p values from Student's t-test shown). Mean is represented by horizontal line. (*G*) Average speed of cells on microposts in a chemokine gradient. Speed was significantly reduced with actomyosin inhibitors, but not PTX. (*H*) Chemotactic index, which is calculated as displacement in the direction of the gradient divided by total path length, with a time-dependent correction (see the Supporting Material). Actomyosin inhibitors show a modest decrease that does not achieve statistical significance but trends in that direction, whereas PTX greatly decreases directional migration. (*I*) The cell spread area is increased with blebbistatin and PTX treatment. The greater area of PTX-treated cells explains why there is no significant difference in total cellular force versus control, despite a significantly lower average force per post. For panels *G–I*, $N = 10$ per condition and error bars represent standard error of the mean. (*Asterisk*) $p < 0.01$.

Consequently, the characteristic timescale of their traction forces are much smaller. DCs exert transient forces, releasing the substrate soon after the leading edge has passed. In our studies, cells engaged an average of 5.5 posts with a force of at least 0.4 nN at any given time. To measure the timescale of this interaction, we examined individual post

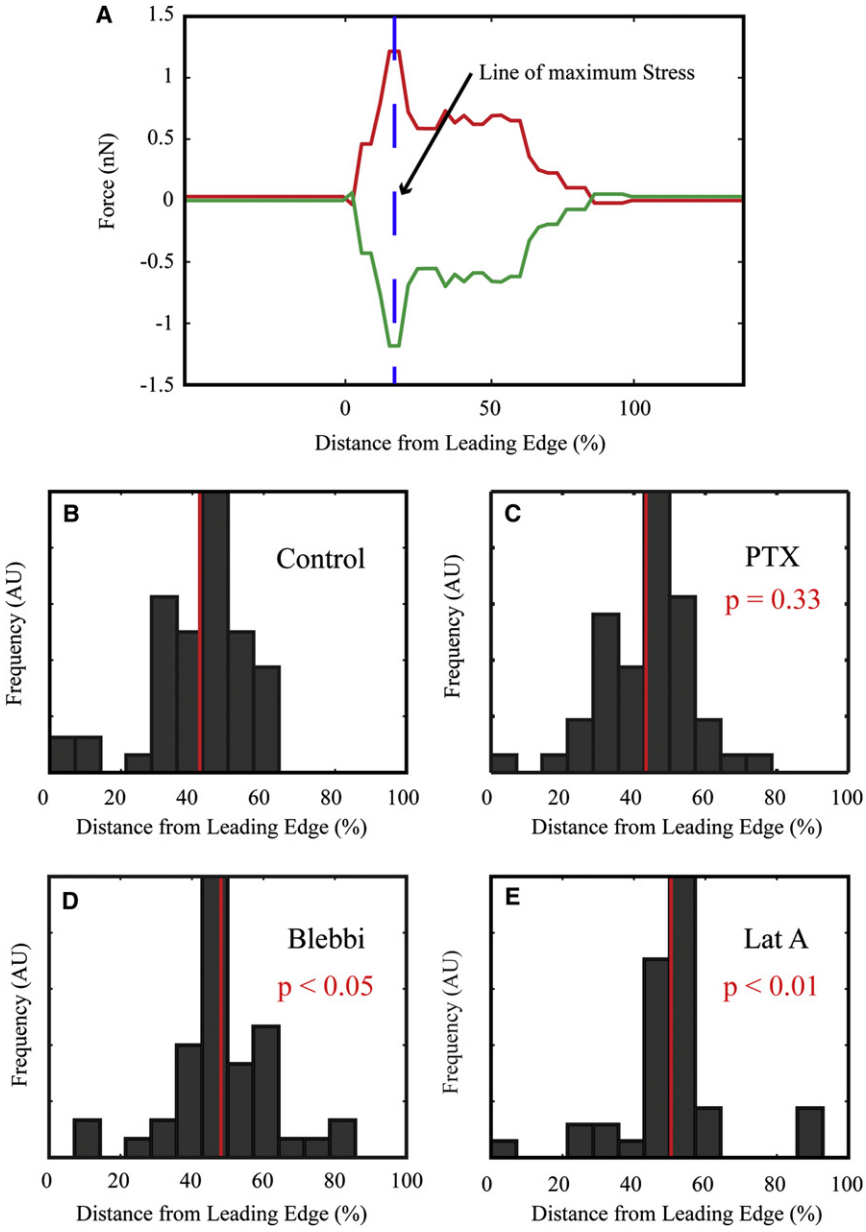

FIGURE 3 Line of maximal stress (LMS) is found in front of the cell centroid. (*A*) Scanning the axis of migration of a typical cell, forces are summed ahead of (*red line*) and behind (*green line*) each point along the axis. The LMS is where the difference in forces is the greatest. (*B*) The LMS is generally found in front of the cell centroid. Data are shown as a histogram of the intersection of the LMS and the axis of migration. The intersections are measured from the leading edge and scaled to the cell length. (*C*) PTX treatment does not affect the average position of the LMS-axis intersection. (*D* and *E*) Actomyosin inhibitors result in a random distribution of LMS-axis intersections. $N = 10$ per condition. Student's *t*-test used to calculate p values versus control.

deflections as the DC leading edge approached, bound, and released the post (Fig. 5, *A* and *B*). Because the post deflections resemble a pulse waveform, the characteristic timescale (τ) was determined using a full-width, half-max analysis of the force profile over time (Fig. 5 *C*). By accumulating data from posts at the leading edge of many cells and fitting to a log-normal distribution ($\mu = 0.85$, $\sigma = 0.72$), we found an average lifetime (τ) of 3.0 min with a median of 2.3 min. Deflection durations sometimes extended to over 6 min and these longer durations were associated with greater maximum forces exerted on the post. In general, τ and F_{max} are correlated (Fig. 5 *E*), indicating a constant rate of energy input from the cell. In the relatively fast-moving DC, the greatest forces under the leading edge have a characteristic lifetime that is determined by the magnitude of force the cell applies to the substrate.

CONCLUSION

Microfluidic devices have become popular for delivering stable chemotactic gradients to cells (33–36). Other methods for inducing chemotaxis, such as transwell assays (37), Zigmond chambers (38), and under-agarose assays (39) rely on transient gradients that make them difficult to optimize. Similarly, micropost arrays have become popular for measuring traction forces due to their relatively simple fabrication and fidelity of results (21). Their higher sensitivity allowed characterization of subtle traction forces that could not be resolved by polyacrylamide gel technology. However,

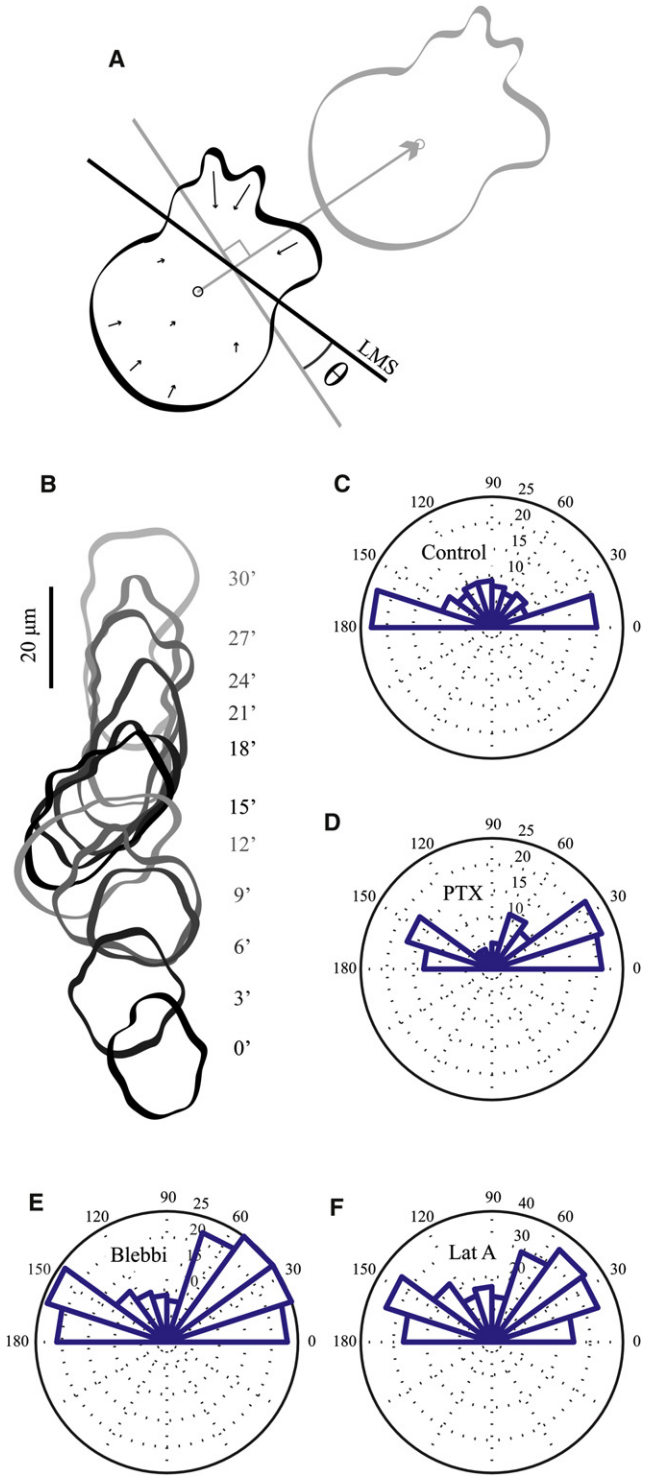

FIGURE 4 Single traction map can be used to predict the direction of migration. (*A*) Schematic of cell migration. Traction forces (*small solid arrows*) are interrogated to find the line of maximal stress (LMS, *solid line*) over the entire cell. The vector (*shaded arrow*) from the cell centroid (*small solid circle*) to the centroid 3 min later (*small shaded circle*) defines the actual direction of motion. The angle θ is defined by the LMS and the vector normal to the direction of motion. (*B*) A typical trajectory of a DC undergoing chemotaxis up a gradient of CCL19 over 30 min. Cell outlines are shown every 3 min. (*C*) A histogram of θ for untreated cells migrating on a micropost array. The LMS closely approximates the line normal to the direction of motion as indicated by a clustering of θ near 0 and 180°. (*D*) Even in cells treated with PTX, the LMS can be used to approximate the direction of motion. (*E* and *F*) Blebbistatin or Latrunculin A treatment decreases the accuracy of predicting the direction of motion. $N = 10$ per condition.

no direct comparison has been made between results on polyacrylamide gels and micropost arrays to determine what effects the differing geometries may have on resultant force profiles. In this work, we combine the microfluidic device and mPADs to measure DC-substrate stresses in an optimized chemotactic gradient. This type of multiplatform technology for accurately measuring the relationship between force and chemotactic signaling will become increasingly important for elucidating the fundamental mechanisms of cellular migration.

Although the molecular machinery for migration is shared across several subtypes of mammalian cells, traction force profiles vary among cell types (12,13,15). The majority of research on cell-substrate forces has focused on strongly adhesive cell types, such as fibroblasts (15,18,19), smooth muscle cells (20), epithelial cells (21–23), endothelial cells (24,25), and stem cells (26). Amoeboid cells represent a distinct type of migration that does not use focal adhesions, but rather rapidly remodels the cell shape to achieve locomotion (4). As an extreme, it has been shown that some leukocytes are capable of migrating in the absence of integrin-based adhesion (3). Although subsequent work has shown that integrins are used in DC motility (2,7,41), no description of traction stresses of dendritic cells has been published until now. We present the first, to our knowledge, traction force maps for DCs showing that these cells concentrate their forces at the leading edge or filopodia. This force profile differs from that of the neutrophil, another leukocyte subtype, which moves by generating squeezing forces in the uropod (12). The short-lived forces exerted by DC at the leading edge are reminiscent of the forces generated at nascent adhesions in mesenchymal cells. However, the similarity ends there as mesenchymal cells generate stable pulling forces at the lamella behind the leading edge and detachment forces at the uropod (12,13,16,28).

Lämmermann et al. (3) have shown that DCs are capable of migrating in the absence of integrins in vitro and in vivo. Although this result is remarkable, subsequent studies have shown that there are substantial differences in migration when integrins are present (2,42), and that TNF-α activated DCs employ a β_2 integrin-dependent mode of transmigration through lymphatic endothelium (6). Additionally, studies on collagen may be misleading because bone marrow DCs are able to adhere to fibronectin, but not collagen (see the Supporting Material), possibly because they express the α_5, α_V, and β_2 integrin subunits (3) for binding fibronectin (43), but not the α_1, α_2, or α_{11} subunits required for binding collagen.

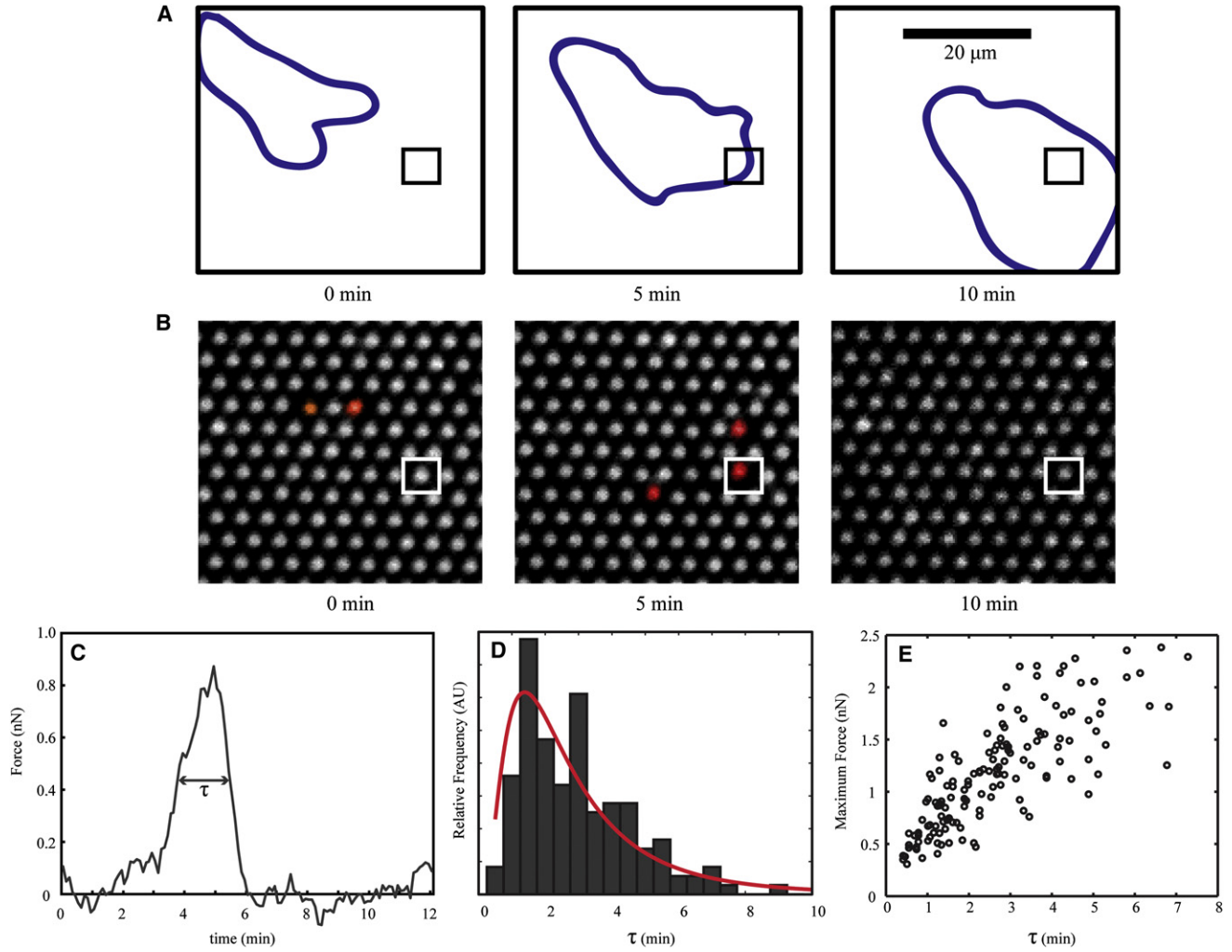

FIGURE 5 Temporal analysis of dendritic cell traction forces. (*A*) Dendritic cells deflect microposts under the leading edge. The cell outline was traced from a phase contrast image (*blue line*). The location of a representative micropost is identified (*black square*) as the cell approaches, binds, and releases the post at 0, 5, and 10 min. Scale bar represents 20 μm. (*B*) Red-channel fluorescence images of microposts at time points corresponding to the traces in panel *A*. (Deflected posts are *pseudo-colored red* for emphasis.) The micropost of interest is tugged as the leading edge passes, then is released when underneath the cell. (*C*) A profile of the magnitude of force on the micropost boxed in panels *A* and *B*. A max-height full-width analysis is used to determine the characteristic duration (τ) of force application. (*D*) The frequency distribution of τ calculated over 144 microposts ($N = 10$). The data fit a log-normal distribution (*red line*) with a mean of 3.0 min and median of 2.3 min. (*E*) The duration of magnitude of force on a post are correlated. As the characteristic time τ increases, the maximum force reached also increases, suggesting a constant energy output from the cell.

Because DCs have a characteristic force profile, we investigated whether migration direction could be predicted from a single force map. In DCs, because the greatest forces are generated at the leading edge, the line of maximal stress is generally found in front of the cell centroid. Additionally, by searching for the global axis of maximal stress, we were able to accurately predict the direction of migration on timescales shorter than the persistence time. Indeed, even when an external gradient could not be sensed due to PTX treatment, the direction of migration could still be predicted. When actomyosin inhibitors are used, the forces are greatly reduced and the axis of maximal stress is a less meaningful predictor.

Migrating cells make use of a spectrum of adhesions to link actomyosin machinery to extracellular substrates. These start as nascent adhesions (44) that may disassemble or mature into focal complexes that may further mature into focal adhesions (45,46). Amoeboid cells will often displace a cell diameter or more within minutes, so they must rely on short-lived nascent-type adhesions whereas mesenchymal cells form focal adhesions that last on the order of hours (47,48). In our system we find that the characteristic timescale for DC adhesion-based traction forces is 2–3 min, indicating that DCs likely use only nascentlike adhesions, but it remains to be seen what similarities and differences exist between these adhesions and nascent adhesions in

mesenchymal cell types. Additionally, we find that the duration and magnitude of the force are positively correlated, indicating that the work rate of the cell is constant during post deflection. This may indicate that the molecular clutch (49) between retrograde actin flow and the adhesion is operating in an all-on or all-off mode.

To reach T cells in secondary lymphoid organs, mature dendritic cells must migrate through peripheral tissue, occasionally cross basement membranes, enter lymphatics, and navigate lymphoid tissue in an integrin-mediated fashion (6,42). Despite the requirement of integrins for parts of DC migration, to our knowledge no traction force maps have been produced until now. We show here that in addition to actin-based polymerization and myosin-based contraction, DCs are able to use short-lived integrin-based adhesions in leading filopodia to effect migration. Understanding these forces and the pathways that generate them leads us one step closer to being able to manipulate them for therapeutic value.

SUPPORTING MATERIAL

Additional narrative with two figures, and five movies, are available at http://www.biophysj.org/biophysj/supplemental/S0006-3495(11)01082-4.

The authors thank Eric Johnston and Beena John for technical support and Colin Choi for helpful discussions.

We acknowledge support from National Institutes of Health grants AI082292 and EB001046. B.G.R. received support from a Merck & Co. graduate fellowship. M.T.Y. received support from the National Science Foundation Integrative Graduate Education and Research Traineeship program (DGE-0221664).

REFERENCES

1. Alvarez, D., E. H. Vollmann, and U. H. von Andrian. 2008. Mechanisms and consequences of dendritic cell migration. *Immunity.* 29:325–342.
2. Schumann, K., T. Lämmermann, …, M. Sixt. 2010. Immobilized chemokine fields and soluble chemokine gradients cooperatively shape migration patterns of dendritic cells. *Immunity.* 32:703–713.
3. Lämmermann, T., B. L. Bader, …, M. Sixt. 2008. Rapid leukocyte migration by integrin-independent flowing and squeezing. *Nature.* 453:51–55.
4. Renkawitz, J., K. Schumann, …, M. Sixt. 2009. Adaptive force transmission in amoeboid cell migration. *Nat. Cell Biol.* 11:1438–1443.
5. Lämmermann, T., and M. Sixt. 2009. Mechanical modes of 'amoeboid' cell migration. *Curr. Opin. Cell Biol.* 21:636–644.
6. Johnson, L. A., and D. G. Jackson. 2010. Inflammation-induced secretion of CCL21 in lymphatic endothelium is a key regulator of integrin-mediated dendritic cell transmigration. *Int. Immunol.* 22:839–849.
7. Lämmermann, T., J. Renkawitz, …, M. Sixt. 2009. Cdc42-dependent leading edge coordination is essential for interstitial dendritic cell migration. *Blood.* 113:5703–5710.
8. Lombardi, M. L., D. A. Knecht, …, J. Lee. 2007. Traction force microscopy in *Dictyostelium* reveals distinct roles for myosin II motor and actin-crosslinking activity in polarized cell movement. *J. Cell Sci.* 120:1624–1634.
9. Uchida, K. S. K., T. Kitanishi-Yumura, and S. Yumura. 2003. Myosin II contributes to the posterior contraction and the anterior extension during the retraction phase in migrating *Dictyostelium* cells. *J. Cell Sci.* 116:51–60.
10. Lee, J., M. Leonard, …, K. Jacobson. 1994. Traction forces generated by locomoting keratocytes. *J. Cell Biol.* 127:1957–1964.
11. Burton, K., J. H. Park, and D. L. Taylor. 1999. Keratocytes generate traction forces in two phases. *Mol. Biol. Cell.* 10:3745–3769.
12. Smith, L. A., H. Aranda-Espinoza, …, D. A. Hammer. 2007. Neutrophil traction stresses are concentrated in the uropod during migration. *Biophys. J.* 92:L58–L60.
13. Shin, M. E., Y. A. He, …, F. Wang. 2010. Spatiotemporal organization, regulation, and functions of tractions during neutrophil chemotaxis. *Blood.* 116:3297–3310.
14. Wang, Y. L. 1984. Reorganization of actin filament bundles in living fibroblasts. *J. Cell Biol.* 99:1478–1485.
15. Beningo, K. A., M. Dembo, …, Y. L. Wang. 2001. Nascent focal adhesions are responsible for the generation of strong propulsive forces in migrating fibroblasts. *J. Cell Biol.* 153:881–888.
16. Dembo, M., and Y. L. Wang. 1999. Stresses at the cell-to-substrate interface during locomotion of fibroblasts. *Biophys. J.* 76:2307–2316.
17. Galbraith, C. G., and M. P. Sheetz. 1997. A micromachined device provides a new bend on fibroblast traction forces. *Proc. Natl. Acad. Sci. USA.* 94:9114–9118.
18. Yang, M. T., N. J. Sniadecki, and C. S. Chen. 2007. Geometric considerations of micro- to nanoscale elastomeric post arrays to study cellular traction forces. *Adv. Mater.* 19:3119–3123.
19. Munevar, S., Y. L. Wang, and M. Dembo. 2001. Traction force microscopy of migrating normal and H-Ras transformed 3T3 fibroblasts. *Biophys. J.* 80:1744–1757.
20. Tan, J. L., J. Tien, …, C. S. Chen. 2003. Cells lying on a bed of microneedles: an approach to isolate mechanical force. *Proc. Natl. Acad. Sci. USA.* 100:1484–1489.
21. Lemmon, C. A., N. J. Sniadecki, …, C. S. Chen. 2005. Shear force at the cell-matrix interface: enhanced analysis for microfabricated post array detectors. *Mech. Chem. Biosyst.* 2:1–16.
22. du Roure, O., A. Saez, …, B. Ladoux. 2005. Force mapping in epithelial cell migration. *Proc. Natl. Acad. Sci. USA.* 102:2390–2395.
23. Trepat, X., M. R. Wasserman, …, J. J. Fredberg. 2009. Physical forces during collective cell migration. *Nat. Phys.* 5:426–430.
24. Reinhart-King, C. A., M. Dembo, and D. A. Hammer. 2003. Endothelial cell traction forces on RGD-derivatized polyacrylamide substrata. *Langmuir.* 19:1573–1579.
25. Nelson, C. M., R. P. Jean, …, C. S. Chen. 2005. Emergent patterns of growth controlled by multicellular form and mechanics. *Proc. Natl. Acad. Sci. USA.* 102:11594–11599.
26. Ruiz, S. A., and C. S. Chen. 2008. Emergence of patterned stem cell differentiation within multicellular structures. *Stem Cells.* 26:2921–2927.
27. Saunders, R. L., and D. A. Hammer. 2010. Assembly of human umbilical vein endothelial cells on compliant hydrogels. *Cell. Mol. Bioeng.* 3:60–67.
28. Jannat, R. A., G. P. Robbins, …, D. A. Hammer. 2010. Neutrophil adhesion and chemotaxis depend on substrate mechanics. *J. Phys. Condens. Matter.* 22:194117.
29. Fu, J. P., Y. K. Wang, …, C. S. Chen. 2010. Mechanical regulation of cell function with geometrically modulated elastomeric substrates. *Nat. Methods.* 7:733–736.
30. Ricart, B. G., B. John, …, D. l A. Hammer. 2011. Dendritic cells distinguish individual chemokine signals through CCR7 and CXCR4. *J. Immunol.* 186:53–61.
31. Riol-Blanco, L., N. Sánchez-Sánchez, …, J. L. Rodríguez-Fernández. 2005. The chemokine receptor CCR7 activates in dendritic cells two signaling modules that independently regulate chemotaxis and migratory speed. *J. Immunol.* 174:4070–4080.

32. Oakes, P. W., D. C. Patel, …, J. X. Tang. 2009. Neutrophil morphology and migration are affected by substrate elasticity. *Blood.* 114:1387–1395.

33. Li Jeon, N., H. Baskaran, …, M. Toner. 2002. Neutrophil chemotaxis in linear and complex gradients of interleukin-8 formed in a microfabricated device. *Nat. Biotechnol.* 20:826–830.

34. Jeon, N. L., S. K. W. Dertinger, …, G. M. Whitesides. 2000. Generation of solution and surface gradients using microfluidic systems. *Langmuir.* 16:8311–8316.

35. Lin, F., and E. C. Butcher. 2006. T cell chemotaxis in a simple microfluidic device. *Lab Chip.* 6:1462–1469.

36. Irimia, D., S.-Y. Liu, …, M. C. Poznansky. 2006. Microfluidic system for measuring neutrophil migratory responses to fast switches of chemical gradients. *Lab Chip.* 6:191–198.

37. Boyden, S. 1962. The chemotactic effect of mixtures of antibody and antigen on polymorphonuclear leucocytes. *J. Exp. Med.* 115:453–466.

38. Zigmond, S. H. 1977. Ability of polymorphonuclear leukocytes to orient in gradients of chemotactic factors. *J. Cell Biol.* 75:606–616.

39. Nelson, R. D., P. G. Quie, and R. L. Simmons. 1975. Chemotaxis under agarose: a new and simple method for measuring chemotaxis and spontaneous migration of human polymorphonuclear leukocytes and monocytes. *J. Immunol.* 115:1650–1656.

40. Reference deleted in proof.

41. Eich, C., I. J. M. de Vries, …, A. Cambi. 2011. The lymphoid chemokine CCL21 triggers LFA-1 adhesive properties on human dendritic cells. *Immunol. Cell Biol.* 89:458–465.

42. Quast, T., B. Tappertzhofen, …, W. Kolanus. 2009. Cytohesin-1 controls the activation of RhoA and modulates integrin-dependent adhesion and migration of dendritic cells. *Blood.* 113:5801–5810.

43. Humphries, J. D., A. Byron, and M. J. Humphries. 2006. Integrin ligands at a glance. *J. Cell Sci.* 119:3901–3903.

44. Choi, C. K., M. Vicente-Manzanares, …, A. R. Horwitz. 2008. Actin and α-actinin orchestrate the assembly and maturation of nascent adhesions in a myosin II motor-independent manner. *Nat. Cell Biol.* 10:1039–1050.

45. Parsons, J. T., A. R. Horwitz, and M. A. Schwartz. 2010. Cell adhesion: integrating cytoskeletal dynamics and cellular tension. *Nat. Rev. Mol. Cell Biol.* 11:633–643.

46. Gardel, M. L., I. C. Schneider, …, C. M. Waterman. 2010. Mechanical integration of actin and adhesion dynamics in cell migration. *In* Annual Review of Cell and Developmental Biology, *Vol. 26*. Annual Reviews Inc., Palo Alto, CA. 315–333.

47. Burridge, K., K. Fath, …, C. Turner. 1988. Focal adhesions: transmembrane junctions between the extracellular matrix and the cytoskeleton. *Annu. Rev. Cell Biol.* 4:487–525.

48. Ridley, A. J., and A. Hall. 1992. The small GTP-binding protein rho regulates the assembly of focal adhesions and actin stress fibers in response to growth factors. *Cell.* 70:389–399.

49. Mitchison, T., and M. Kirschner. 1988. Cytoskeletal dynamics and nerve growth. *Neuron.* 1:761–772.